



1 *Conference Proceedings Paper*

## 2 **Estimation of sunflower yields at a decametric spatial** 3 **scale - A statistical approach based on multi-temporal** 4 **satellite images**

5 **Remy Fieuzal<sup>1,\*</sup>, Vincent Bustillo<sup>1,2</sup>, David Collado<sup>2</sup> and Gerard Dedieu<sup>1</sup>**

6 <sup>1</sup> Centre d'Études de la BIOSphère (CESBIO), Université de Toulouse, CNES/CNRS/INRA/IRD/UPS,  
7 Toulouse, France; gerard.dedieu@cesbio.cnes.fr

8 <sup>2</sup> IUT Paul Sabatier, 24 rue d'Embaquès, Auch, France; vincent.bustillo@iut-tlse3.fr;  
9 david.collado@univ-tlse3.fr

10 \* Correspondence: fieuzal.remy@gmail.com; Tel.: +xx-xxx-xxx-xxxx

11 Published: date

12 Academic Editor: name

13 **Abstract:** Recent advances in sensors onboard harvesting machines allow accessing the intra-plot  
14 variability of yields, spatial scale fully compatible with numerous on-going satellite missions. The  
15 aim of this study is to estimate the sunflower yield at the intra-plot spatial scale using the  
16 multi-temporal images provided by the Landsat-8 and Sentinel-2 missions. The proposed approach  
17 is based on a statistical algorithm, testing different sampling strategies to partition the dataset into  
18 independent training and testing sets: a random selection (testing different ratio), a systematic  
19 selection (focusing on different plots), and a forecast procedure (using an increasing number of  
20 images). Emphasis is put on the use of high spatial and temporal resolution satellite data acquired  
21 throughout two agricultural seasons, on a study site located in southwestern France. Ground  
22 measurements consist in intra-plot yields collected by a surveying harvesting machine with GPS  
23 system on track mode. The forecast of yield throughout the agricultural season provides early  
24 accurate estimation two months before the harvest, with  $R^2$  equal to 0.59 or 0.66 and RMSE of 4.7 or  
25 3.4 q ha<sup>-1</sup>, for the agricultural seasons 2016 and 2017 respectively. Results obtained with the random  
26 selection or the systematic selection will be developed later, in a longer paper.

27 **Keywords:** sunflower; yield estimates; forecast; sampling strategy; Landsat-8; Sentinel-2; random  
28 forest  
29

---

### 30 **1. Introduction**

31 Over the last 50 years, the world production and the areas allocated to sunflower have both  
32 increased steadily, with positive trends of around 0.6 million tones and 0.4 million hectares per year,  
33 respectively (trends derived from the statistics of [1]). In France, the culture occupies a large part of  
34 the useful agricultural area (behind wheat, barley, rapeseed and maize). The spatial distribution of  
35 the sunflower is highly disparate considering a department benchmark. With an average of 75,000  
36 hectares in the last ten years, the Gers department ranks first, gathering more than 10% of the  
37 national area allocated to sunflower [2]. In view of the considered surfaces, the challenge is to  
38 identify suitable tools to monitor the culture, able to meet the constraints related to the crop growth  
39 cycle (agricultural season for several months) and the organization of the landscape (irregular and  
40 fragmented parcels).

41 The surface observation capabilities provided by the satellite missions constitute a useful tool,  
42 allowing to access to repetitive information on the surface states. They are conditioned by the

43 characteristics of the embedded sensors operating in specific wavelengths (*e.g.*, visible, near or  
44 medium infrared, thermal or microwave) and delivering products at different spatial scales (pixel  
45 sizes ranging from meters to several kilometers). The contribution of satellite imagery for the  
46 monitoring of agricultural areas has been previously demonstrated, as evidence by the large range of  
47 applications dealing with various topics as the classification of land uses, the monitoring of the crop  
48 or the soil status (through the estimation of target parameters), the mapping of cultural practices or  
49 the detection of crop damage zones [3-5]. In the context of yield estimates, optical images have been  
50 widely used, providing a regular status of the photosynthetic activity of canopy. Estimates of yields  
51 were obtained using different approaches at spatial scale ranging from the region to the field [6-7].  
52 Nevertheless only few studies deal with the monitoring of intra-plot variability of yields and rarely  
53 with the real-time aspect.

54 The objective of this study is to take both advantage of optical decametric satellite missions (by  
55 combining acquisitions performed by Landsat-8 and Sentinel-2A) together with ground data  
56 collected by sensors onboard harvesting machines to estimate yields of sunflower at the intra-plot  
57 scale (*i.e.*, spatial resolution of 30 m). The network of plots where ground measurements and satellite  
58 data were available is fully described in section 2. The proposed approach is based on random forest,  
59 considering reflectance as predictive variables and crop yields as target. The results are analyzed  
60 and discussed (sections 3 and 4), focusing on the estimates throughout the agricultural season which  
61 addresses the potential of real-time estimates.

## 62 2. Experiments

### 63 2.1. Materials

#### 64 2.1.1. Study site

65 The study area is located in southwestern France in the Gers County. Surrounded by valleys,  
66 the territory is characterized by a great diversity of landscapes and types of soil comprising ustic  
67 luvisols, limestone, clay-limestone or more sandy soils. The county is subject to oceanic and  
68 mediterranean climatic influences, with a precipitation regime spatially and annually variable. The  
69 useful agricultural area occupies 71% of the territory (or 447 223 ha), being mainly dedicated to the  
70 cultivation of seasonal crops (cereal for 44.5% or oleaginous and proteinaceous for 24%) or forage  
71 crops and evergreen surfaces for 19% [2]. The present paper focuses on sunflower, for which the  
72 agricultural season delineated by the sowing and harvesting periods is observed from spring to  
73 autumn.

#### 74 2.1.2. Intra-plot yield data

75 A network of 12 and 10 field plots of sunflower (representing 117 and 140 hectares (ha)  
76 respectively) were monitored to collect agricultural practices and the value of yields from farmers,  
77 during two successive agricultural seasons. Sizes of these fields ranged from 3.2 to 28.6 ha. The  
78 sunflower was sown during the spring, mostly during the month of April, and was harvested during  
79 the month of September. The mean values of yield ranged from 18.1 to 31.0 q ha<sup>-1</sup> for 2016 and from  
80 and 16.9 to 24.1 q ha<sup>-1</sup> for 2017, showing a variability depending on the considered plot, as evidence  
81 by the coefficients of variation (*i.e.*,  $CV = 100 \times \text{standard deviation} / \text{mean}$ ) ranged from 18 to 36%.

82 The yield values were derived from the data collected by the surveying harvesting machine  
83 with GPS system on track mode, namely the distance, the width of the cutting bar, the flux and the  
84 humidity of grain. The distance and the width of the cutting bar were first combined to obtain the  
85 area matching with the grain flux. The harvested yields were then computed and dry yields were  
86 last calculated by accounting for the humidity of grain. All the measurements performed in a pixel  
87 with a spatial resolution of 30 m were aggregated, avoiding the extreme values (*i.e.*, average plus  
88 three sigma or 99.7% of the values). Those maps of yields constitute the targeted variable of the  
89 statistical algorithm.

90 2.1.3. Optical satellite images

91 Table 1 presents an overview of the satellite images acquired during the two agricultural  
 92 seasons. From April to September, regular high spatial resolution images were provided by  
 93 Sentinel-2 (4 and 11 images for the years 2016 and 2017 respectively) and Landsat-8 (6 images for the  
 94 year 2016).

95 **Table 1.** Characteristics of the satellite remote sensing data

Years	2016		2017
Satellites	Sentinel-2	Landsat-8	Sentinel-2
Dates (M-D)	05-21 ; 06-20	04-15 ; 06-09 ; 07-04	04-06 ; 05-06 ; 05-16
	07-10 ; 07-30	08-12 ; 09-06 ; 09-13	05-26 ; 06-05 ; 06-25
			07-05 ; 08-04 ; 08-14 08-24 ; 09-13

96

97 The time series of Landsat-8 and Sentinel-2 images were provided by the Theia land data center.  
 98 The images were processed using the software developed by [8], delivering level 2A products  
 99 characterized by ortho-rectified surface reflectance. The data were first corrected from atmospheric  
 100 effects and provided with a mask of clouds and their shadows on the ground (using a  
 101 multi-temporal algorithm). All the images were finally resized at the same spatial resolution of 30 m.

102 In the present study, focus is on the comparable bands considering the wavelength, that is  
 103 signals acquired in blue, green, red, near infrared and short wavelength infrared. The satellite  
 104 images constitute the input data of the statistical algorithm described hereinafter, considering two  
 105 cases: the widely used Normalized Difference Vegetation Index or the combination of the six  
 106 reflectances.

107 2.2. Methods

108 The multi-temporal satellite acquisitions are used to estimate the yields throughout the  
 109 agricultural season of crops. Beginning with the first image acquired after the period of sowing  
 110 (April), the estimates are then performed with a cumulative number of successive images (*i.e.*, 1 to 10  
 111 or 11 images for the years 2016 and 2017, respectively), until the harvest of crops (September). For  
 112 each estimation of yields, the dataset is partitioned into independent training and testing sets, using  
 113 a ratio of 50/50.

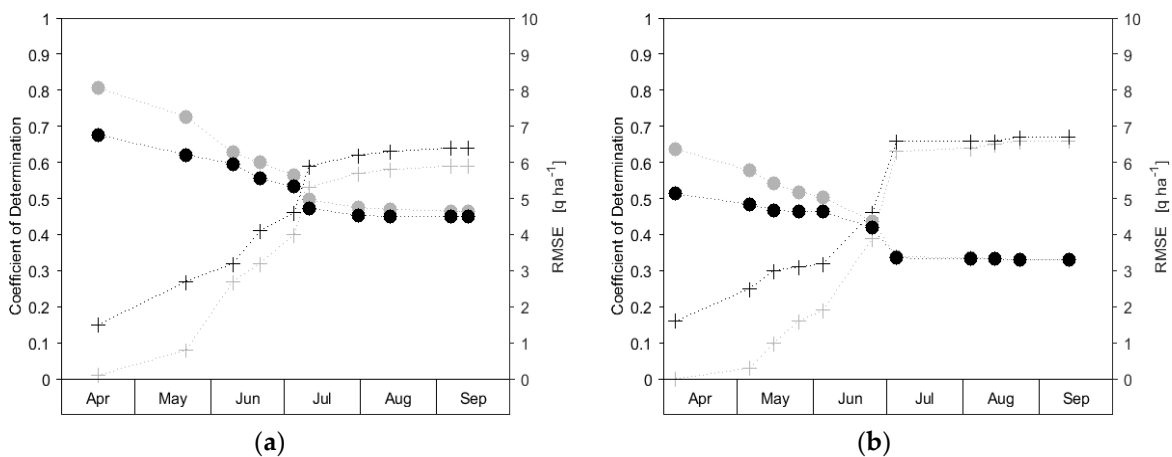
114 The estimation of yield is based on the statistical algorithm proposed by [9]. Random forest has  
 115 been widely used in different fields providing accurate estimates of both qualitative (through  
 116 classification) and quantitative (through regression) variables. This non-parametric approach  
 117 consists in combining an ensemble of independent decision trees trained on different set of samples,  
 118 through a procedure called bagging (abbreviation of bootstrap aggregating). Each decision tree is  
 119 first trained on a subset of randomized samples derived from the initial dataset using bootstrap  
 120 procedure, and used to provide estimates for the remaining independent samples. The decision trees  
 121 are finally aggregated through the weighted mean of the ensemble of estimations, providing an  
 122 estimate of the targeted variable. Unlike other statistical methods that may have limitations related  
 123 to problems of over-adjustment, noise influence on data, or stability of results, random forests are  
 124 particularly appropriate in multi-factorial context to account for non-linear relationships.

125 Coefficient of determination ( $R^2$ ) and root mean square error (RMSE) are finally derived from  
 126 the comparison between the observed and estimated yields. The analysis of results presented in the  
 127 following section focuses on the independent testing set. Similar procedure was tested using  
 128 artificial neural networks, showing slightly lower performances For the sake of conciseness, only  
 129 results obtained using random forest are presented hereinafter.

130 **3. Results**

131 *3.1. Multi-temporal estimation of yields*

132 The temporal evolution of statistical indexes associated to the yield retrieval is illustrated for  
 133 the years 2016 and 2017 (Figure 1 a and b respectively), focusing on estimates based on NDVI and on  
 134 the combination of different satellite reflectances. The statistical performance observed throughout  
 135 the crop's agricultural season shows comparable general behavior, regardless the year or the satellite  
 136 data considered. A strong increase of accuracy is first observed with the cumulative number of  
 137 satellite acquisitions used for estimating yields. In 2016, the 6 images acquired from April to July  
 138 (days 106 to 192) allow the  $R^2$  to increase from 0.15 to 0.59, while RMSE decrease from 6.7 to 4.7  $q.h^{-1}$   
 139 (considering the estimates based on the 6 reflectances). In 2017, 7 images are acquired during the  
 140 same period (days 96 to 186) and statistics show higher performances, the  $R^2$  increasing from 0.16 to  
 141 0.66 and RMSE decreasing from 5.1 to 3.4  $q.h^{-1}$ . However, a notable difference is observed between  
 142 the two considered years regarding the gain of accuracy. Indeed, the gain appears progressive in  
 143 2016, while the maximal increase is associated to the two images acquired at the end of June and at  
 144 the start of July in 2017(days 176 and 186). Such behavior is closely related to the growth dynamic of  
 145 sunflower, which can vary from one year to the other through the combination of agricultural  
 146 practices (especially the dates of sowing) and climatic conditions (e.g., cold or warm conditions  
 147 which can reduce or accelerate the growth rate). Then, performances saturate at specific  
 148 phenological stage (flowering), and only slight gain of accuracy is obtained by the addition of new  
 149 satellite images.

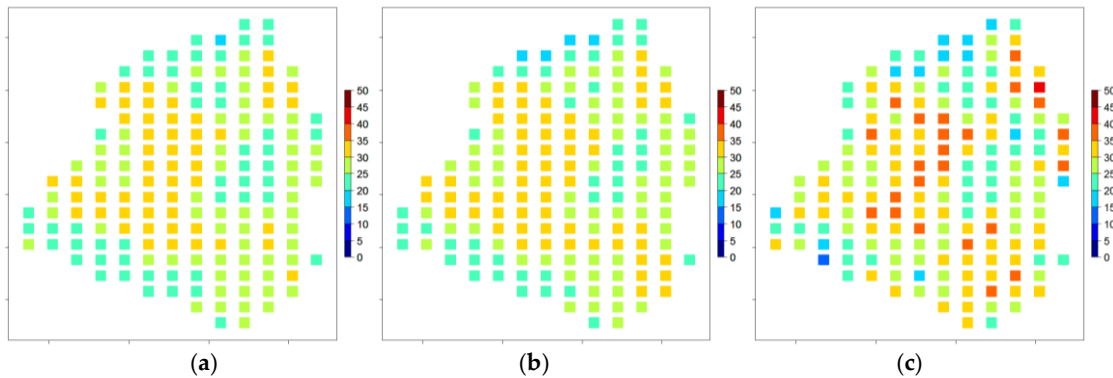


150 **Figure 1.** Temporal evolution of the statistical performance (coefficients of determination and root  
 151 mean square errors, crosses and dots respectively) associated to sunflower yield forecast using NDVI  
 152 (in grey) or the combination of six reflectances (in black), for the years 2016 (left) and 2017 (right).

153 *3.2. Mapping of yields at the intra-plot spatial scale*

154 Finally, two maps of yield obtained during the agricultural season 2016 are compared to the  
 155 intra-plot measurements (Figure 2). The estimated maps of yield observed during the months of July  
 156 and September are derived from the 6 or 10 successively acquired images, respectively. The maps  
 157 present similar intra-plot spatial patterns of low and high values of yield, and only few difference  
 158 are observed between estimates performed two months before the harvest and those obtained just  
 159 before the harvest (differences inferior to 2.8  $q.ha^{-1}$ , with a mean value of 0.7  $q.ha^{-1}$ ). Such  
 160 observation is confirmed considering all the pixel of the plot through the values of the averages of  
 161 estimated yields (28.1 and 28.5  $q.ha^{-1}$ ), the standard deviations (3.2 and 3.2  $q.ha^{-1}$ ), or the range (from  
 162 20.0 to 33.3  $q.ha^{-1}$  and 20.2 to 34.1  $q.ha^{-1}$ ). These two maps provide accurate estimates of the targeted  
 163 variable (with relative error lower than 13% compared to measurements), nevertheless similar bias

164 are observed, that is, extreme low and high measured values are not well reproduced by the  
165 statistical approach.



166

167 **Figure 2.** Maps of sunflower yield estimated two months before the harvest (a) and just before the  
168 harvest (b), together with measurements (c) collected on a plot dedicated to the cultivation of  
169 sunflower in 2016.

#### 170 4. Discussion

171 The ability of obtaining accurate early estimates of yield has been demonstrated in previous  
172 agronomic studies focused on wheat or corn [10-12]. Interesting performance are thus observed  
173 during specific crop phenological stages, *i.e.*, during the elongation of the main stem of wheat or  
174 when the central stem of corn develops. For the sunflower, the accurate in-season estimates are  
175 observed during the first half of July, whatever the considered year. During this period, the fields  
176 cultivated with sunflower are observed at two characteristic phenological stages (BBCH scale  
177 numbers 5 and 6, [13]), corresponding to the inflorescence emergence and flowering. Moreover, the  
178 in-season performance observed for sunflower appear consistent with other studies based on the use  
179 of successive acquired optical and radar image [14,15], even if the yield estimates are not performed  
180 at the same spatial scale (intra-scale scale in the present study *vs.* field scale in the previous papers).  
181 In those studies, the levels of accuracy depend on both the considered crop (*e.g.*,  $R^2 = 0.76$  and  $RMSE$   
182  $= 7.0 \text{ q ha}^{-1}$  for wheat,  $R^2$  of 0.69 and an  $RMSE$  of  $7.0 \text{ q ha}^{-1}$  for corn) and on the configuration of the  
183 satellite signals used as input variable of the statistical algorithm (*i.e.*, several combinations of  
184 frequencies and polarizations combinations were tested). Nevertheless, the statistics were obtained  
185 with a limited number of ground truth (due to the difficulty to obtain precise information on yield,  
186 the number of fields  $\sim 30$ ) and for a single agricultural season. In the present study, the robustness of  
187 the approach is tested considering two agricultural seasons and large dataset of more than thousand  
188 of measurements for each studied year.

#### 189 5. Conclusions

190 The proposed study addresses the potential of using multi-temporal optical images (Landsat-8  
191 and Sentinel-2A) for the estimation of sunflower yields at the intra-plot spatial scale. The statistical  
192 approach takes advantage of both regular decametric satellite images acquired throughout two  
193 agricultural seasons and yield measurements collected on a network of plots. Random forest are  
194 implemented on independent training and testing sets, considering a forecast of yield throughout  
195 the agricultural season.

196 In the present study, the data were collected by a surveying harvesting machine with GPS  
197 system on track mode which presents the following advantages: (i) the ability of working at a spatial  
198 scale consistent with the size of pixels and thus considering the intra-field variations of yield (which  
199 are merged when working at the field or at the regional scale), and (ii) obtaining a large dataset,  
200 useful for testing the robustness of the proposed approaches (*i.e.*, the algorithm being trained and  
201 validated on more than one thousand of measurements). Moreover, the proposed approaches were

202 solely based on series of optical satellite images and tested on two successive agricultural seasons,  
203 showing comparable trends and stability of the results regarding the levels of accuracy.

204 The estimation of yield throughout the agricultural season provide a demonstration of the  
205 potential of real-time approaches by considering an increasing number of successive satellite images.  
206 Accurate in-season estimation of yields were observed two months before the harvest ( $R^2$  of 0.59 or  
207 0.66 and RMSE of 4.7 or 3.4 q ha<sup>-1</sup> for the years 2016 and 2017). Moreover, the map of yield obtained  
208 during the crop flowering presented spatial patterns consistent with those estimated just before  
209 harvest (correlation close to 0.96 between the two estimated maps).

210 **Acknowledgments:** The authors wish to thank the Theia land data center for providing the level 2A Landsat-8  
211 and Sentinel-2 satellite images. In addition, the authors wish to thank the agricultural cooperative AGRO D'OC,  
212 especially Mrs. Guigues, Mr. Gambini and Mr. Hypolite, for their time and precious discussion, and the farmers  
213 who helped to collect the ground data.

## 214 References

- 215 1. Food and Agriculture Organization of the United Nations or FAO. Available online: <http://faostat.fao.org/>  
216 (accessed on 25 February 2019).
- 217 2. Agreste. Available online: <http://agreste.agriculture.gouv.fr/> (accessed on 25 February 2019).
- 218 3. Fieuzal, R.; Baup, F. Estimation of leaf area index and crop height of sunflowers using multi-temporal  
219 optical and SAR satellite data. *Int. J. Remote Sens.* **2016**, *37*, 2780–2809.
- 220 4. Marais Sicre, C.; Inglada, J.; Fieuzal, R.; Baup, F.; Valero, S.; Cros, J.; Huc, M.; Demarez, V. Early detection  
221 of summer crops using high spatio-temporal resolution optical images time series. *Remote Sens.* **2016**, *8*,  
222 591.
- 223 5. Yang, H.; Chen, E.; Li, Z.; Zhao, C.; Yang, G.; Pignatti, S.; Casa, R.; Zhao, L. Wheat lodging monitoring  
224 using polarimetric index from RADARSAT-2 data. *Int. J. Appl. Earth Obs. Geoinf.* **2015**, *34*, 157–166.
- 225 6. Fieuzal, R.; Marais Sicre, C.; Baup, F. Estimation of sunflower yield using a simplified agrometeorological  
226 model controlled by optical and SAR satellite data. *IEEE J. Sel. Top. Appl. Earth Observ. Remote Sens.* **2017**,  
227 *10*, 5412–5422.
- 228 7. Becker-Reshef, I.; Vermote, E.; Lindeman, M.; Justice, C. A generalized regression-based model for  
229 forecasting winter wheat yields in Kansas and Ukraine using MODIS data. *Remote Sens. of Environ.* **2010**,  
230 *114*, 1312–1323.
- 231 8. Hagolle, O.; Huc, M.; Villa Pascual, D.; Dedieu, G. A Multi-Temporal and Multi-Spectral Method to  
232 Estimate Aerosol Optical Thickness over Land, for the Atmospheric Correction of FormoSat-2, LandSat,  
233 VENμS and Sentinel-2 Images. *Remote Sens.* **2015**, *7*, 2668–2691.
- 234 9. Breiman, L. Random forests. *Mach. Learn.* **2001**, *45*, 5–32.
- 235 10. Bushong, J.T.; Mullock, J.L.; Miller, E.C.; Raun, W.R.; Klatt, A.R.; Arnall, D.B. Development of an in-season  
236 estimate of yield potential utilizing optical crop sensors and soil moisture data for winter wheat. *Precis.*  
237 *Agric.* **2016**, *17* (4), 451–469.
- 238 11. Sharma, L.K.; Franzen, D.W. Use of corn height to improve the relationship between active opticals sensor  
239 readings and yield estimates. *Precis. Agric.* **2014**, *15*, 331–345.
- 240 12. Yin, X.; Hayes, R.M.; McClure, M.A.; Savoy, H.J. Assessment of plant biomass and nitrogen nutrition with  
241 plant height in early-to mid-season corn. *J. Sci. Food Agric.* **2012**, *92*, 2611–2617.
- 242 13. Meier, U. Stades Phénologiques des Mono- et Dico-tylédones Cultivées. Centre Fédéral de Recherches  
243 Biologiques pour l'Agriculture et les Forêts, 2001. [www.agroedieurope.fr/ref/doc/BBCH.pdf](http://www.agroedieurope.fr/ref/doc/BBCH.pdf)
- 244 14. Fieuzal, R.; Baup, F. Forecast of wheat yield throughout the agricultural season using optical and radar  
245 satellite images. *Int. J. Appl. Earth Obs. Geoinf.* **2017**, *59*, 147–156.
- 246 15. Fieuzal, R.; Marais-Sicre, C.; Baup, F. Estimation of corn yield using multi-temporal optical and radar  
247 satellite data and artificial neural networks. *Int. J. Appl. Earth Obs. Geoinf.* **2017**, *57*, 14–23.

